SURFACE DISPLACEMENT MONITORING OF SUBURBAN EXPRESSWAY UNDER CONSTRUCTION BASED ON SENTINEL-1 SBAS-INSAR ANALYSIS

X.Q. Qin [1], Y.J. Huang [1], X.G. Shi [2 *], L.F. Xie [3], X.S. Chen [1]

[1] School of Civil and Traffic Engineering & Underground Polis Academy, Shenzhen University, Shenzhen, 518060, China
[2] School of Geography and Information Engineering, China University of Geosciences, 430074, China
[3] Smart City Research Institute & School of Architecture and Urban Planning, Shenzhen University, 518060, China

KEY WORDS: Suburban expressway, SBAS-InSAR, Structure, Slope, Subgrade, Soil yard.

ABSTRACT:

The Synthetic Aperture Radar Interferometry (InSAR) technique can quickly obtain millimeter-level surface deformation in urban areas with high coherence. However, expanding the application of time series InSAR in non-urban areas is an important research focus. An improved SBAS-InSAR analysis approach is applied in this study to present the surface displacement along two expressways under construction. Taking the Kejiao and Yicheng Highway in the Shenzhen Shanwei Special Cooperation Zone as examples, the deformation along the highways under construction and the surrounding ground objects is revealed. Moreover, the time series displacements and construction conditions are combined to explain the possible mechanisms behind the different displacements of various ground objects along the expressways. The results show that the climate, environment, and construction conditions of the cooperation zone had an impact on the deformation of various ground objects along the route. Compared to traditional PS-InSAR methods, the density and accuracy of coherence points are improved, which better overcomes the spatiotemporal incoherence effects in non-urban areas.

1. INTRODUCTION

The Synthetic Aperture Radar Interferometry (InSAR) technique can quickly obtain millimeter-level surface deformation in urban areas with high coherence (Liao et al., 2020; Qin et al., 2021; Cai et al., 2022). However, expanding the application of time series InSAR in non-urban areas is an important research focus. Summarizing the current research progress, the current problems lie in the inaccurate identification and integration of structural PTs in non-urban areas, and lacking detailed deformation analysis of different areas around under-constructing expressways (Shami et al., 2022; Xing et al., 2022; Ge et al., 2020). Firstly, the coherence of expressways under construction in non-urban areas is influenced by continuous construction and complex non-urban environment, making it difficult to select dense and accurate point-like targets (PTs) along the expressway structure. Secondly, the previous studies always ignore the environment-structure coupling analysis, leaving the detailed deformation analysis of different expressway construction periods still unclear.

An improved SBAS-InSAR analysis approach is applied in this study to present the surface displacements along the Kejiao and Yicheng expressways in the Shenzhen Shanwei Special Cooperation Zone under construction. The results indicate that there were severe settlements in the soil yard along the highway, and the surrounding artificial slopes and buildings generally remain stable, while the embankment experienced slight settlement. The time series displacements and construction conditions are combined to explain the possible mechanisms behind the different displacements of various ground objects along the expressways. The results show that the climate, environment, and construction conditions of the cooperation zone had an impact on the deformation of various ground objects along the route.

2. STUDY AREA AND DATASETS

2.1 Study Area

Shenzhen Shanwei Special Cooperation Zone is located in the west of Shanwei City, Guangdong Province, at the easternmost end of the Guangdong-Hong Kong-Macao Greater Bay Area, with a total area of 468.3 km^2. The original landform of the research area is mainly hills. Due to the late development and construction, most of the surface of the cooperation zone are still be covered with vegetation in 2023, making it a typical non-urban area. Since the implementation of the overall development plan for the cooperation zone in November 2014, the local area has ushered in a wave of large-scale construction of infrastructure such as roads and buildings. The Kejiao and Yicheng are two important expressways connecting the north and south of the cooperation zone, both of which are designed with eight lanes in both directions. Their construction periods began in September and December 2019 respectively, and are expected to be completed by the end of 2023, with a construction period of three years.

2.2 Datasets

To study the surface displacement along the road under construction, the cooperation zone's Kejiao and Yicheng Expressway were selected as the research objects. To avoid the loss of coherence caused by a long research period, 59 ascending Sentinel-1A images from January 2021 to December 2022 were collected for deformation monitoring. The main parameters of the data are shown in Table 1.

* Corresponding author

Parameter	Description
Date	2021 Jan~2022 Dec 10:25
Number of Images	59
Relative Orbit	113
Mode	IW
Pass Direction	Ascending
Polarisation	VV
Band	C
Average Incidence Angle	39.4 °

Table 1. Sentinel-1A image parameters of the study area

3. METHODOLOGY

An improved SBAS-InSAR analysis approach is applied in this study to present the surface displacement along two expressways under construction. Considering that changes in ground features caused by the construction process can easily lead to low coherence or even loss of coherence, a shorter spatiotemporal baseline was set to balance accuracy and the number of coherent points. The final time baseline threshold is set to 48d, and the spatial baseline threshold is 150m. The SBAS interference combination is shown in Figure 1. Among them, the 40th, 52nd, 53rd, and 56th scene images only obtain 1-2 pairs of image matching due to the large spatial baseline deviation, and most images can meet an average of 4 or more interference combinations.

Since the undulating terrain and lush vegetation of the study area may have significant impacts on the terrain and water vapor phase, the 30m SRTM v3 DEM and GACOS processing module were introduced in this study to eliminate the errors of the terrain phase and water vapor phase. The minimum cost flow method of the triangular network was used for phase unwrapping (Delaunay MCF), and a linear model was used for the inversion of surface displacement.

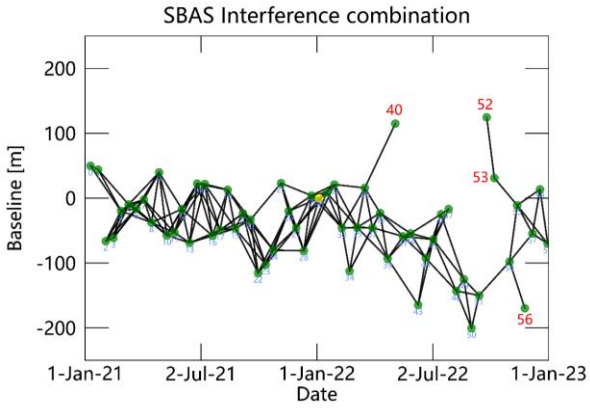

Figure 1. SBAS interference combination

4. OVERALL DEFORMATION ANALYSIS AND VALIDATION

The distribution of the main features along the road under construction is shown in Figure 2, which can be roughly divided into '4S', (structures, slopes, soil yards, and subgrades). The deformation monitoring results derived from the traditional PS-InSAR method and the improved SBAS method used in this study are illustrated in Figure 2 (b) and (c). Regarding the distribution of PTs, the high coherent PTs in Figure 2 (b) are only distributed on some sparse artificial buildings. The improved SBAS method obtained more point targets through shorter spatiotemporal baseline combinations, especially along two highways (as shown in Figure 2 (c)), which will support more reliable deformation analysis and interpretation.

To facilitate the description of the changing states of various ground features, the deformation was artificially divided into five levels based on LOS velocity and represented in different colors in Figure 3. The dark blue represents points with slight uplift (V_{LOS}>5mm/yr), which is expressed as the 'S-U'; Light blue represents the relative stable points ($V_{LOS} \in$ [-5,5] mm/yr), expressed as the 'Stable'; Light green represents points with slight settlement ($V_{LOS} \in$ [-5, -15] mm/yr), shown as the 'S-S'; Orange represents points with moderate settlement ($V_{LOS} \in$ [-15, -25] mm/yr), shown as the 'M-S'; and Red represents points experienced heavy settlement (V_{LOS}<-25mm/yr), expressed as the 'H-S'. From Figures 2 (c), it can be roughly seen that the internal deformation of the road ranges from slight settlement to slight uplift, while the external buildings are more stable. Moreover, the soil yards along the expressways showed moderate or even heavy settlement.

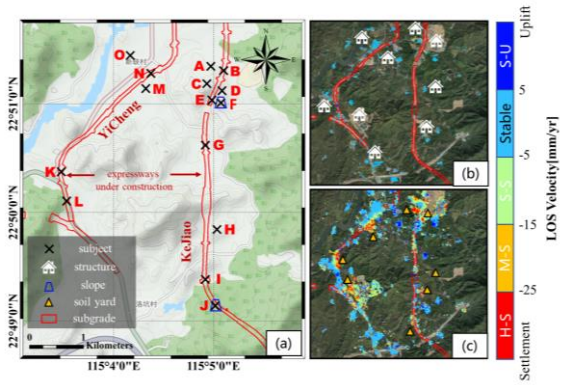

Figure 2. Time series InSAR results and distribution map of terrain along the expressways

Several representative ground objects with high densities of coherent points (see A~O in Figure. 2 (a)) were taken as observation objects, as shown in Figure. 3. Among them, a marked the position of a ground control point (GCP) of the Kejiao expressway with a black target symbol. The annual elevation re-measurement results from 2020 to 2023 showed that the displacement rate of the GCP was 0.000mm/yr, and the closest coherent point to the GCP as well as the PTs within a radius of 20m were taken for comparison, as shown in Table 2. The differences in LOS velocity obtained by the nearest neighbor method and the 20m arithmetic mean method during the observation period were about 0.142mm/yr and 0.102mm/yr, respectively, demonstrating the mm-level monitoring accuracy of the results in this study.

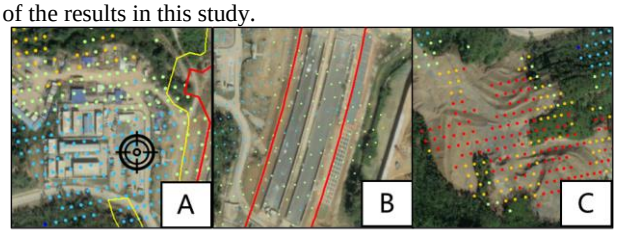

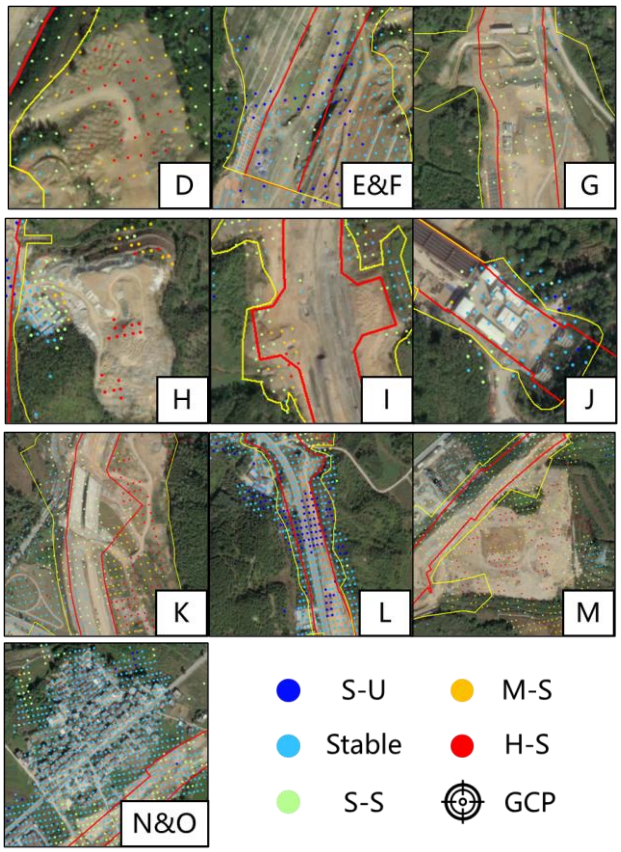

Figure 3. Satellite imagery and distribution of coherent points of main ground objects

Comparison method	Coherence coefficient		V_{LOS} [mm/yr]	
	Mean	standard deviation	Mean	standard deviation
Nearest	0.743	0	0.142	0
Within 20m	0.772	0.050	0.102	0.424

Table 2. Accuracy verification statistics

The features in Figure 3 are divided into four categories, including the buildings (A and O), road embankments (B, E, G, I, L, and N), soil yard along the road (C, D, H, and M), and slopes (F, J, and K). To display a more detailed summary of the position, deformation state, and LOS velocity of various features in Figure 3, we made a statistics of coherent point on each type of objects, as is illustrated in Table 3.

Object	Position	State	LOS Velocity [mm/yr]	
			mean	range
Concrete Structure	O	Stable	1.8	-4.8～4.4
Steel Structure	A	Stable	0.5	-4.4～5.0
Natural Slope	K	H-S	-25.6	-60.7～-7.4
Engineering Slope	J	Stable	0.9	-2.8～6.3
Soil Slope	F	Stable	2.3	-6.6～9.0
Spoil Ground	C, D, H	H-S	-35.1	-78.7～-7.6
Flat Area	M	H-S	-25.4	-49.3～-15.5
Cutting Subgrade	E, L	Stable	3.4	-10.6～11.6
Embankment Subgrade	B, N	S-S	-5.8	-13.3～-1.8
Soft-soil Subgrade	G	S-S	-10.6	-23.3～2.0
Backfilling Subgrade	I	M-S	-20.9	-28.7～-15.5

Table 3. Statistical of LOS Velocity and Overall Status of Various Ground Objects

From distribution and magnitude of LOS_Velocity at coherent points, the position A is the most stable, showing the smallest deformation rate and fluctuation range. While C, D, and H exhibited the largest and most unstable sedimentation rate and fluctuation range. From the perspective of deformation rate, there are no features in the S-U state. In the stable state, steel structure building A < engineering slope J < concrete structure building O < soil slope F < cutting subgrade E and L. In the S-S state, embankment subgrade B, N < soft-soil subgrade G. In the M-S state, there is only secondary backfilling of roadbed I. In the H-S state, the Flat area M ≈ natural slope K < spoil ground C, D, and H.

The average time series displacement curves of coherent points on similar ground features are calculated to represent the overall deformation trend of the slope, soil yard, structure, and subgrade along the highway, as shown in Figure 4. It can be seen that the overall settlement of the building remains stable, while the slope and subgrade generally show a stable or slight settlement trend, and the exposed soil exhibits severe settlement. This is also consistent with the deformation statistics and analysis from Table 3.

According to the curve in Figure 4, the curves corresponding to the 53rd scene showed significant uplift. Moreover, the displacement curves corresponding to the 40th, 52nd, 53rd, and 56th scene images with poor interference combination in Figure 1 showed significant fluctuations (marked by red dashed lines), and the fluctuation direction is basically consistent with the spatial baseline offset direction. On the other hand, the time series curves of the four types of land features showed similar time of peaks and valleys, with only varying amplitudes, which may indicate that the fluctuations of the time series curve are influenced by the changes of the spatial baseline. The similar fluctuations in the mean curve can be considered as systematic errors caused by baseline offset, and excessively small surface true displacements are easily masked by the fluctuations caused by the spatial baseline. Therefore, the main focus will be on the trend changes of the curve in the subsequent analysis, and the

similar fluctuations of all ground features in the same direction will be ignored.

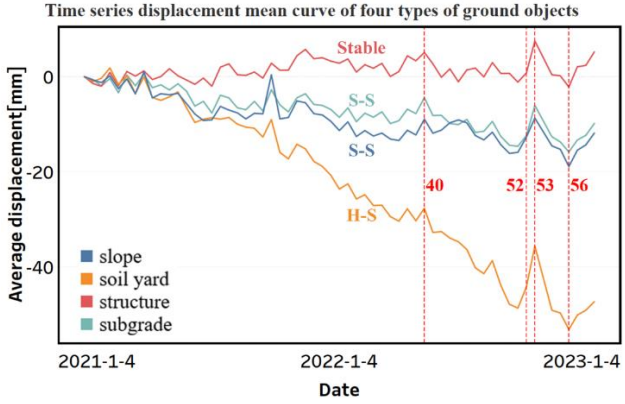

Figure 4. Time series mean curves of four types of ground objects.

The average temperature and monthly rainfall data for each month in the Shenzhen Shanwei Cooperation Zone from January 2021 to December 2022 is shown in Figure 5. The statistical results of rainfall and temperature in different seasons are shown in Table 4. In the winter of 2021-2022 (December to February of the following year), the average monthly rainfall is 43.5mm, and the average monthly temperature is 21.2 ℃. In spring (March to May), the average monthly rainfall is 66.1mm, and the average monthly temperature is 27.8 ℃. In summer (June to August), the average monthly rainfall is 306.4mm, and the average monthly temperature is 32.3 ℃. In autumn (September to November), the average monthly rainfall is 88.2mm, and the average monthly temperature is 29.8 ℃. Based on the above analysis, the summer rainfall accounts for about 60% of the annual rainfall. Moreover, due to uncertain weather conditions such as typhoons, the total rainfall in 2022 was 2162mm, which is 2.5 times of 2021. The top three months in terms of rainfall were June 2022, August 2022, and June 2021, respectively.

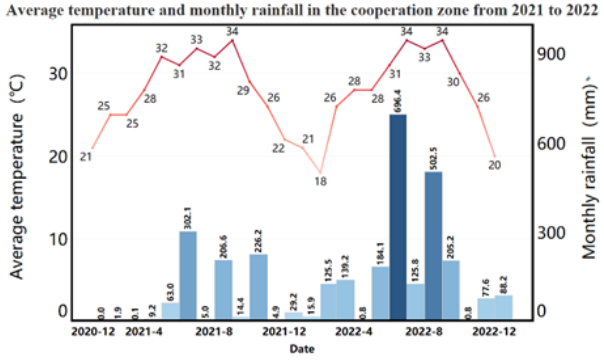

Figure 5. Monthly Average Temperature and Rainfall in Shenshan Cooperation Zone from 2021 to 2022.

Time	Total Rainfall [mm]			Average Temperature
	season	subtotal	total	[°C]
2021	Spring	72.3	958.9	28.3
	Summer	513.7		32
	Automn	245.5		29.7
	Winter	127.4		22.7
2022	Spring	324.1	2162	27.3
	Summer	1324.7		32.7
	Automn	283.6		30
	Winter	229.6		19.7

Table 4. Total rainfall and average air temperature statistics for each season in the cooperation zone from 2021 to 2022

5. DEFORMATION ANALYSIS OF DIFFERENT TYPES OF GROUND FEATURES

5.1 Structure Objects

The structure objects in Figure 3 include the position A and O. Position A is the project station of Kejiao Expressway, which is built in September 2019 and mainly composed of steel structure containers. It is a temporary building with a building area of about 3000 km^2, which is 40m to 250m away from kejiao highway. Position o is a local village that was built earlier and mainly consists of concrete, brick and tile structures. It covers an area of approximately 60000 km^2 and is 50 to 300m away from Yicheng highway.

The time series average displacement curves of position A and O are shown in Figure 6. The abnormal fluctuations in the displacement curve caused by spatial baseline offset are marked with gray dashed lines, the obvious opposite fluctuations are marked with red dashed lines, and the changes of displacement trend are indicated with red or blue solid arrows.

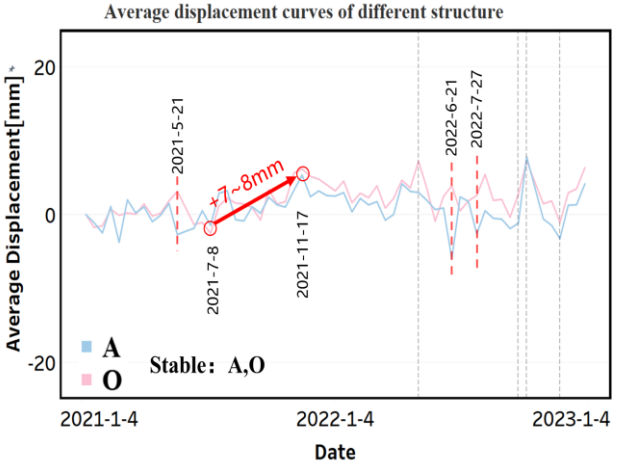

Figure 6. Average displacement curves of different structure.

It can be concluded that the two types of buildings generally maintain a stable state during the observation period, with a slight upward trend from July 8, 2021 to November 17, 2021. After an average upward movement of 7-8mm, they begin to slowly sink and return to a stable state. The fluctuation directions of the observed data on May 21, 2021, June 21, 2022, and July 27, 2022 are significantly opposite. According to historical rainfall data, moderate to high intensity rainfall has been maintained for the first 12 days of June 21, 2021, but the rainfall was not significant during the first 12 days of May 21, 2021 and July 27, 2022. From the perspective of temperature, from May to September 2021, the temperature remained at a high level above 31 ℃. As a result, building materials such as cement, concrete, and steel would accumulate thermal stress and expand, until the temperature dropped to 26 ℃ in

November. From June to October 2022, a high temperature of 30 ℃ was maintained. There is one month lag compare to 2021, the temperature plummeted to 26 ℃ in November. Although the baseline error had animpact on the curve during the same period, it can still be seen that there was an upward trend after June 2022. Observing from the satellite image, the position A and O are respectively located beside the two construction roads of Kejiao and Yicheng, with a distance of about 1km. The impact of Roadworks on the two buildings is independent, but the overall impact is small.

In summary, the buildings along the roads were not significantly affected by construction, but rather were greatly affected by temperature, rainfall, or other factors. The main reason for the uplift of the curve from July to November 2021 was material expansion caused by high temperatures in summer and autumn. The abnormal fluctuations on June 21, 2022 may be affected by sustained heavy rainfall, while the fluctuations on May 21, 2021 and July 27, 2022 may be due to the road construction.

5.2 Slope Objects

The features representing the slopes include F, J, and K in Figure 3. Among them, F is a six-level excavation slope of the kejiao project, with a slope ratio of 1:2.5. It was gradually excavated and formed from 2020 to 2021. Due to the gentle slope, no protective measures were taken after excavation, and the surface is soil. The slope J is located at the tunnel entrance, with a top slope of 1:1 and a gradient of 3:10 towards the foot of the slope. It was excavated and formed in early 2020, with an intercepting ditch set up at the top of the slope, and the slope surface was comprehensively protected by engineering and vegetation, with complete ancillary facilities. Position K is a natural slope with a gentle slope and sparse shrub vegetation covering the surface. It is located close to the bridge of Yicheng, which crosses a tributary of the Chishi River. There are several construction roads directly connect to Yicheng Avenue, making it easy for construction personnel and vehicles to pass through.

The time series displacement curves of slope objects in the study area are shown in Figure 7. Position F and J belong to excavation slopes, and although unloading rebound may occur after excavation, the soil remains stable. K is a natural soil slope, which is generally showing a moderate settlement trend due to the traffic construction of Yicheng and the influence of rivers. Analyzing the impact of temperature (similar to the building objects), the subsidence began to expand under the influence of high-temperature stress from the end of June 2021 until early November. Compared to soil slope F, slope J is affected by temperature later due to engineering protection, manifested as the alternating peaks and valleys of F and J deformation curves between June and August of 2021. The average rise of J affected by high temperature is 9mm, which is smaller than the average rise of f (13mm). Overall, k shows moderate subsidence, where the temperature-induced uplift completely covered by subsidence. However, as shown by the blue arrow in Figure 7, the subsidence amount in the four months before November 5, 2021 is less than that in the following four months.

In terms of rainfall impact, most of the time from May 21, 2021 to June 26, 2021 experienced moderate rain, and even two rainstorms occurred during this period. As soil slopes, F and K are greatly affected during this time, resulting in severe settlement of the curve. However, J has comprehensive drainage and surface protection measures and is not significantly affected by rainfall.

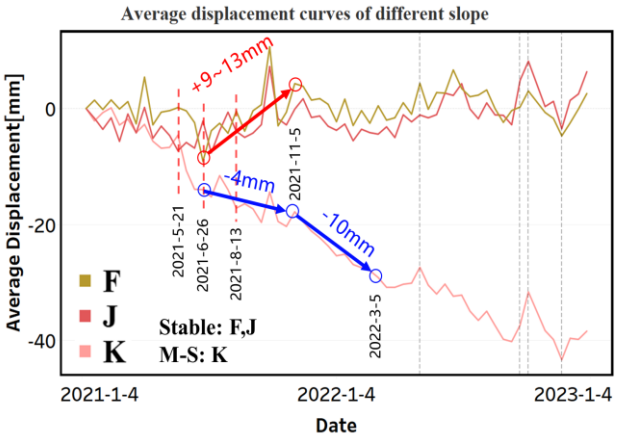

Figure 7. Average displacement curves of different slopes.

In summary, the slope underwent deformation under the influence of temperature, as well as rapid settlement due to rainwater or river erosion. The impact of engineering on the slope is double-sided. The vibration caused by construction may cause instability of the slope. However, comprehensive slope protection can effectively resist the interference caused by external factors on the slope.

5.3 Subgrade Objects

The landmarks represented by B, E, G, I, L, and N in Figure 3 are the subgrades of Kejiao and Yicheng expressways. Their deformation curves are shown in Figure 8.

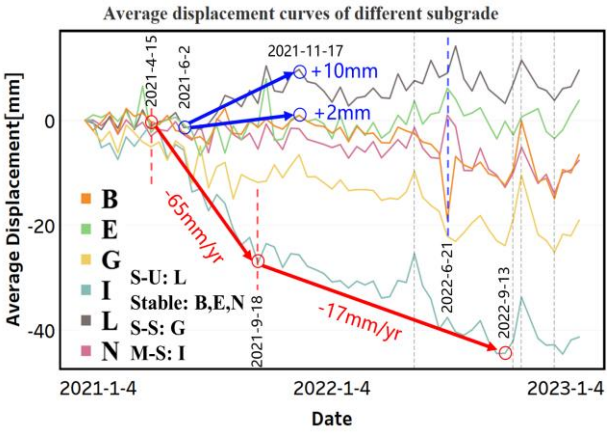

Figure 8. Average displacement curves of different subgrade.

Among them, L and E belong to the excavated roadbed. Due to the use of open excavation to cross the mountain, both sides of the road section are engineering slopes. This type of roadbed is usually relatively sturdy. Based on the satellite image in Figure 3, the slopes on both sides of L are secondary and tertiary slopes. Each standard slope has a height of 8m, and the excavation depth is about 16m. The roadbed still presents a soil color, indicating that it has not been excavated to the rock layer. And on both sides of E, there are six-level and seven-level slopes, respectively, with a depth of over 48m. The roadbed appears grayish brown, indicating that it has entered the rock layer. From the average displacement curves in Figure 8, it can be observed that E and L are generally in a stable state, and are also affected by the increase of temperature in summer. As a result, the soil base layer L is raised by about 10mm, and the rock base layer E is raised by about 2mm. Under similar external environmental conditions, rock layers typically have

better physical properties than soil layers and are less affected by temperature. For example, the subgrade E has been excavated to the rock layer. Geological survey data shows that the rock layer is strongly weathered carbonaceous mudstone, with a grayish brown appearance and a layer thickness of 1.6 to 51.7m. In natural conditions, the bearing capacity is as high as 400kpa, and the cohesion is 28kpa, which is 4.5 times and 2.8 times that of ordinary artificial fill, respectively.

Both B and N are filled subgrade, with drainage facilities such as hidden ditches and side ditches arranged along the road. B has already laid an asphalt pavement, and some protection works have been completed for the embankment slopes on both sides. The two subgrades show a slight subsidence trend, and are not significantly affected by temperature. B and N are adjacent to the building A and building O respectively. On June 21, 2022, A and B, N and O showed similar fluctuations, indicating that the deformation of buildings on that day was probably affected by Roadworks in addition to heavy rainfall. Compared to 12 days ago, the settlement of B increased by 12.7mm, while the settlement of A only increased by 5.1mm. Due to the small impact of rainfall on building A in the curve, it can be considered that this part of settlement fluctuation is completely caused by construction vibration. In addition to construction vibrations, B was also partially affected by rainfall.

The subgrade G is a soft soil subgrade, with the original appearance of a pond. After completing the relocation of the Dawan Creek channel in the north and draining the pond in August 2020, there is still about 30cm of silt left. This part of the silt was not removed, but the roadbed was reinforced by stone throwing and squeezing. Subsequently, the embankment was formed by layered soil covering. Compared to ordinary embankments b and n, the settlement of g is relatively larger, but it still belongs to slight settlement, and not significantly affected by rainfall or temperature.

The subgrade I is located at the planned intersection, and the embankment was excavated twice to lay the horizontal and vertical pipe gallery. It was completed and backfilled in April 2021. From Figure 3(I), it can also be seen that due to the incoherence caused by excavation and backfilling, insufficient coherence points were obtained in the middle of the road. From the displacement curve of subgrade i in Figure 8, a rapid settlement occurred soon after the backfilling from April 2021, until September 2021 when it began to converge. Other external factors such as temperature, the interference is not significant.

5.4 Soil Yard Objects

Features C, D, H, and M are all composed of stacked soil. All of the C, D and H are temporary spoil grounds formed in 2020, with an area of approximately 40000m^2, 19000m^2, and 44000m^2, respectively, which are used to store soil from slope and tunnel excavation. Position M is a flat area, which is constructed on uneven ground to facilitate subsequent urban construction, with an area of approximately 60000 m^2. The formation process of spoil grounds and flat area are similar, both of which are formed by layered compaction of the soil, with the difference being that the flat area is usually larger, while the spoil ground tends to increase the height of the soil pile.

According to the average displacement curves in Figure 9, both the spoil ground and the flat area are in a state of heavy settlement. Due to their complete composition of soil, large catchment areas, and inadequate drainage measures, they are greatly affected by rainfall. As shown by the red arrow in the figure, during June 2021 and June September 2022, the rainfall resulted in a settlement rate (-68~-80mm/yr) significantly greater than normal weather (-25mm/yr, H-S). Moreover, since the duration and total amount of rainfall from June to September in 2022 (about 1530mm) are 2.9 times higher than in 2021 (about 528mm), the average soil settlement caused by the rainfall during these months in 2022 (about 21mm) are almost 3 times severer than that of the same period in 2021 (about 7 mm). After deducting the natural settlement, the contribution of rainfall factors to the settlement of the soil yard is -43~-55mm/yr, and the settlement purely caused by rainfall are approximately 4mm (2021) and 12mm (2022), respectively.

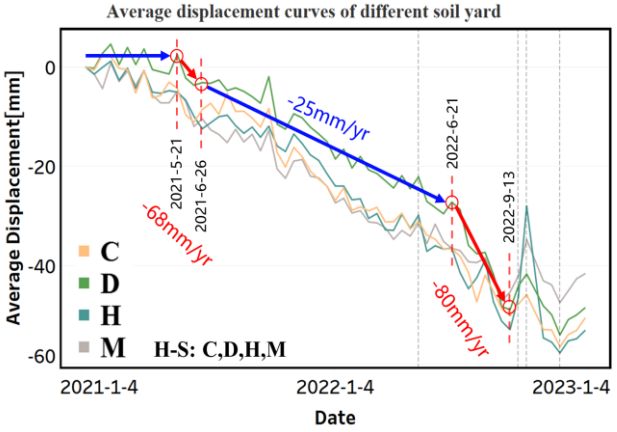

Figure 9. Average displacement curves of different soil yard

6. CONCLUSIONS

In this study, Sentinel-1A images of Shenzhen Shanwei Special Cooperation Zone from 2021 to 2022 were used to process images based on the improved SBAS InSAR method of GACOS, and the distribution of coherent points and the trend of overall deformation of main ground objects along the expressway under construction were classified and discussed, and the temporal changes of various ground objects were analyzed in detail in combination with Satellite imagery, local meteorology and construction process. The main conclusions are as follows:

(1) During the research period and within the study area, various buildings and artificial slopes remained basically stable, the subgrades showed a stable or sinking trend, and the overall settlement of the soil yard was severe. Therefore, attention should be paid to strengthening monitoring.

(2) The continuous high temperatures in summer and autumn will cause the expansion and uplift of building materials and some stable roadbed, with an annual uplift of about 10mm. Rock is the least affected by temperature expansion, followed by steel and concrete, and soil is the most affected by temperature stress, but only 13mm. Due to the small amplitude of temperature deformation, the contribution to the overall trend of subsidence in surface deformation is not significant.

(3) Persistent heavy rainfall usually exacerbates land subsidence, especially on land features with a surface type of soil. The settlement speed of the spoil ground during the rainy season is 3 times that of normal weather, and the settlement is almost proportional to the rainfall.

(4) Engineering protection measures and comprehensive drainage system can effectively resist the negative impact of

high temperature and rainfall on the stability of ground features, but construction itself may also cause deformation and fluctuations of surrounding ground features.

The improved SBAS InSAR method helps to broaden the monitoring application of temporal InSAR in non-urban areas. Although this method can serve as an effective means of monitoring slow ground deformation, we found that for short-term significant changes such as asphalt laying and soil filling, the results obtained by this method are either easily incoherent or not reflected in the time series curve. How to strengthen the monitoring of these changes will be the focus of subsequent work.

ACKNOWLEDGEMENTS

This work is supported by the National Natural Science Foundation of China (Grant No. 42104012), the Shenzhen Science and Technology Program (Grant No. JCYJ20220531101812028), and the program of Shenzhen Key Laboratory of Green, Efficient and Intelligent Construction of Underground Metro Station (Grant No. ZDSYS20200923105200001).

REFERENCES

Cai, J., Liu, G., Jia, H., Zhang, B., Wu, R., Fu, Y., ... & Zhang, R. 2022. A new algorithm for landslide dynamic monitoring with high temporal resolution by Kalman filter integration of multiplatform time-series InSAR processing. *International Journal of Applied Earth Observation and Geoinformation*, 110, 102812.

Ge, P., Gokon, H., Meguro, K. 2020. A review on synthetic aperture radar-based building damage assessment in disaster. *Remote Sensing of Environment*, 240: 111693.

Liao, M., Wang R., Yang M., Wang, N., Qin, X. 2020. Techniques and applications of spaceborne time-series InSAR in urban dynamic monitoring. *Journal of Radars*, 9(3): 409–424.

Qin, X., Li, Q., Ding, X., Xie, L., Wang, C., Liao, M., ... & Xiong, S. 2021. A structure knowledge-synthetic aperture radar interferometry integration method for high-precision deformation monitoring and risk identification of sea-crossing bridges. *International Journal of Applied Earth Observation and Geoinformation*, 103, 102476.

Shami, S., Azar, M. K., Nilfouroushan, F., Salimi, M., & Reshadi, M. A. M. 2022. Assessments of ground subsidence along the railway in the Kashan plain, Iran, using Sentinel-1 data and NSBAS algorithm. *International Journal of Applied Earth Observation and Geoinformation*, 112, 102898.

Xing, X., Zhu, Y., Xu, W., Peng, W., & Yuan, Z. 2022. Measuring Subsidence Over Soft Clay Highways Using a Novel Time-Series InSAR Deformation Model With an Emphasis on Rheological Properties and Environmental Factors (NREM). *IEEE Transactions on Geoscience and Remote Sensing*, 60, 1-19.